Electronic Supplementary Information

$Mg_{0.8}Zn_{0.2}O$ Microspheres: Preparation, Characterization and Application for Degrading Organic Dyes

Yajun Zheng,[a],[b] Liyun Cao,[b]* Gaoxuan Xing,[a] Jianfeng Huang,[b] and Zhiping Zhang[a],[c]*

[a] *School of Chemistry and Chemical Engineering, Shaanxi Province Key Laboratory of Environmental Pollution Control and Reservoir Protection Technology of Oilfields, Xi'an Shiyou University, Xi'an 710065, China; Fax: +86 29 8838 2693; Tel: +86 29 8838 2694; E-mail: zhangzp0304@gmail.com (Z. Zhang).*

[b] *School of Material Science and Engineering, Shaanxi University of Science and Technology, Xi'an 710021, China; E-mail:* caoliyun@sust.edu.cn *(L. Cao).*

[c] *State Key Laboratory of Petroleum Pollution Control, CNPC Research Institute of Safety and Environmental Technology, Beijing 102206, China*

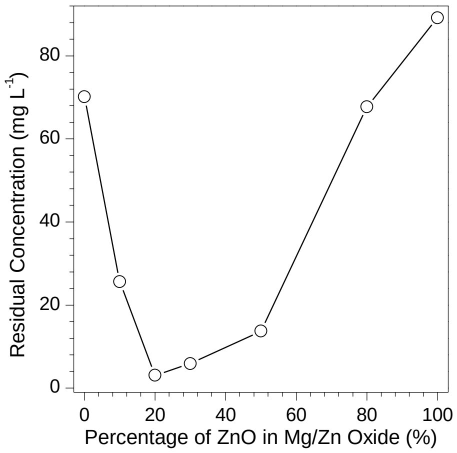

Figure S1. Residual concentration of 300 mg L^{-1} methylene blue aqueous solution after treatment with Mg/Zn binary oxides by varying the molar percentages of $Zn(NO_3)_2$ in preparation (light source: UV light; irradiation period: 90 min).

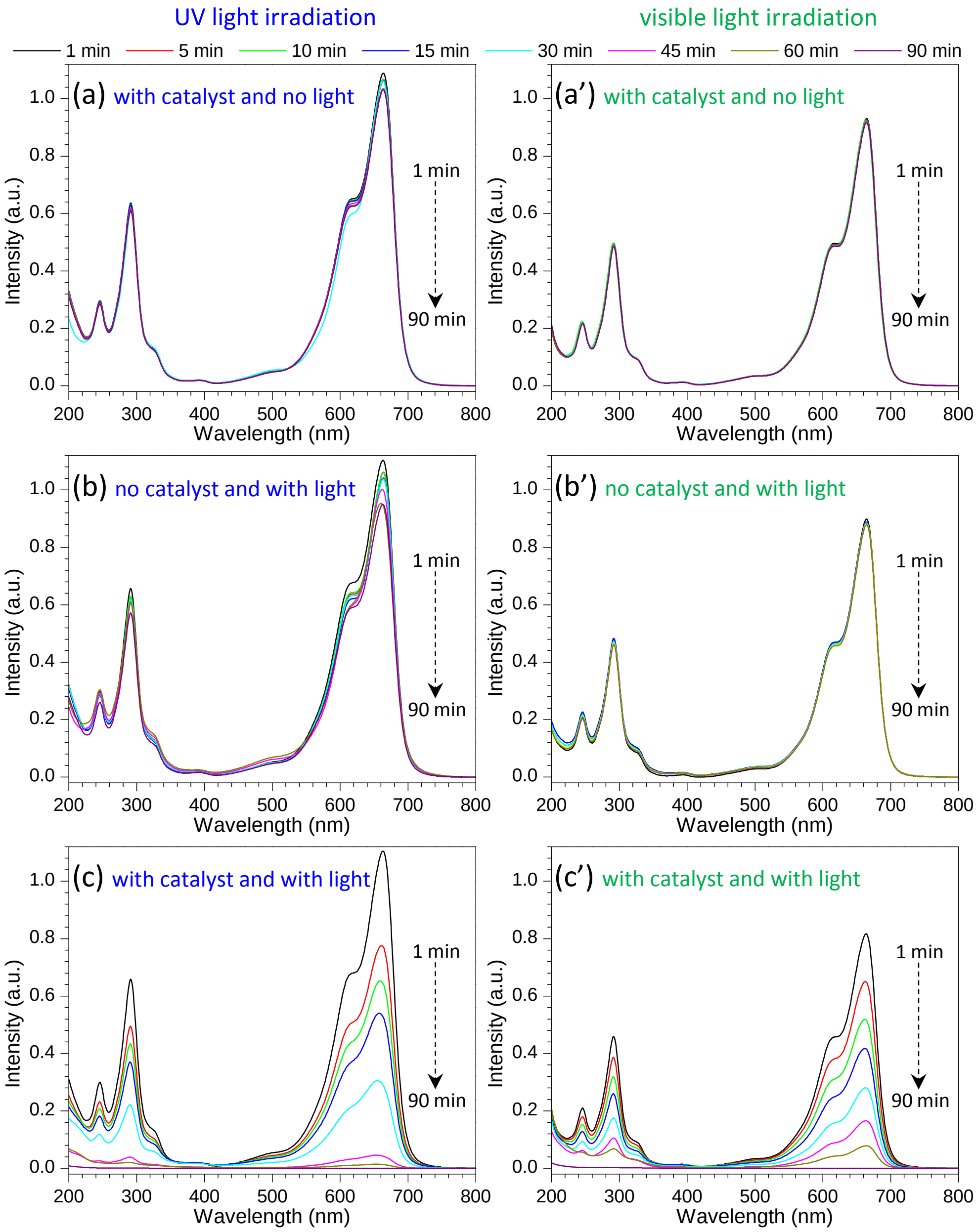

Figure S2. UV-vis spectra of methylene blue aqueous solution after treatment under different conditions as marked upon irradiation in [**(a)**, **(b)** and **(c)**] UV light (initial concentration: 300 mg L^{-1}; solution volume: 50 mL; catalyst amount: 25 mg; irradiation period: 90 min) and [**(a')**, **(b')** and **(c')**] visible light (initial concentration: 100 mg L^{-1}; solution volume: 50 mL; catalyst amount: 50 mg; irradiation period: 90 min). It should be mentioned that for the methylene blue solutions after treatment with UV light, they were diluted 50 times prior to the measurement of UV-visible spectrometer, whereas they were diluted 20 times for the system with visible light irradiation.

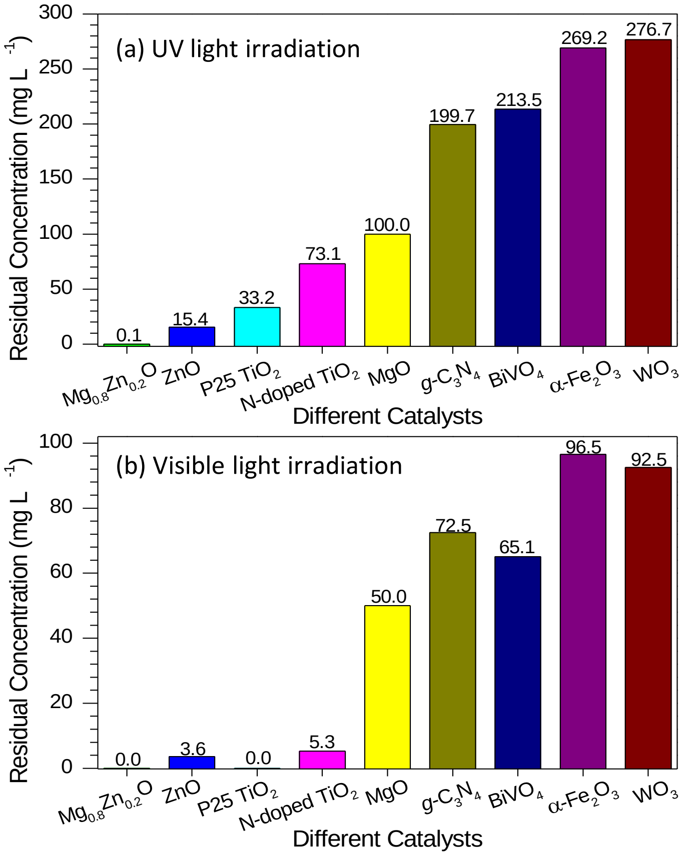

Figure S3. Comparison of the performance of developed spherical $Mg_{0.8}Zn_{0.2}O$ particles with other related state-of-the-art photocatalysts **(a)** in degradation of 50 mL of 300 mg L^{-1} methylene blue aqueous solution upon UV light irradiation (irradiation time: 90 min; catalyst amount: 25 mg; solution pH: 4.39) and **(b)** in degradation of 50 mL of 100 mg L^{-1} methylene blue aqueous solution upon visible light irradiation (irradiation time: 90 min; catalyst amount: 50 mg; solution pH: 5.47).

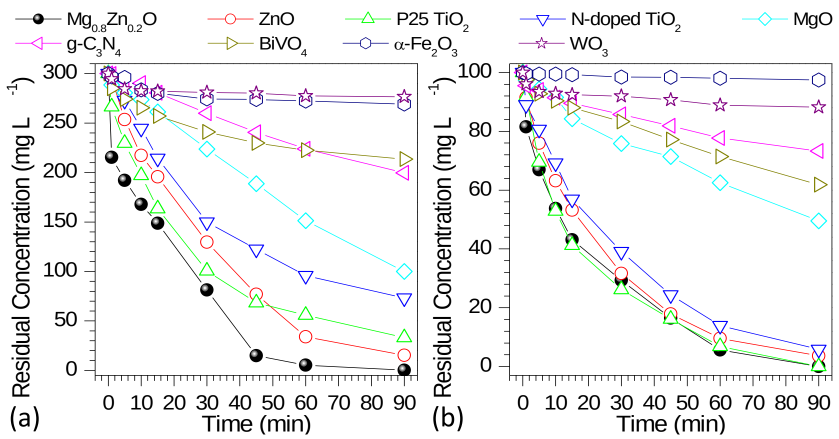

Figure S4. Photocatalytic degradation of MB over various photocatalysts upon irradiation in **(a)** UV light (initial concentration: 300 mg L^{-1}; solution volume: 50 mL; catalyst amount: 25 mg) and **(b)** visible light (initial concentration: 100 mg L^{-1}; solution volume: 50 mL; catalyst amount: 50 mg).

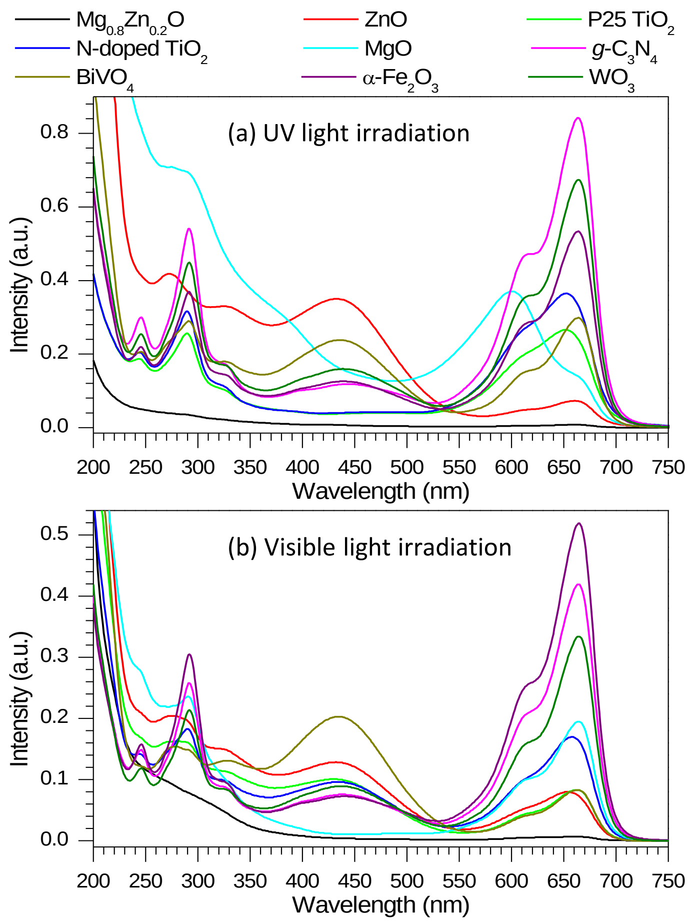

Figure S5. UV-vis spectra of 50 mL mixed dye solution (MB, Congo red, thymol blue, bromothymol blue, and eriochrome black T) being treated with $Mg_{0.8}Zn_{0.2}O$, ZnO, P25 TiO_2, N-doped TiO_2, MgO, *g*-C_3N_4, $BiVO_4$, α-Fe_2O_3, and WO_3 upon irradiation in **(a)** UV light (concentration of each dye: 300 mg L^{-1}; catalyst amount: 25 mg; solution pH: 4.39) and **(b)** visible light (concentration of each dye: 300 mg L^{-1}; catalyst amount: 50 mg; solution pH: 5.47) for 90 min.

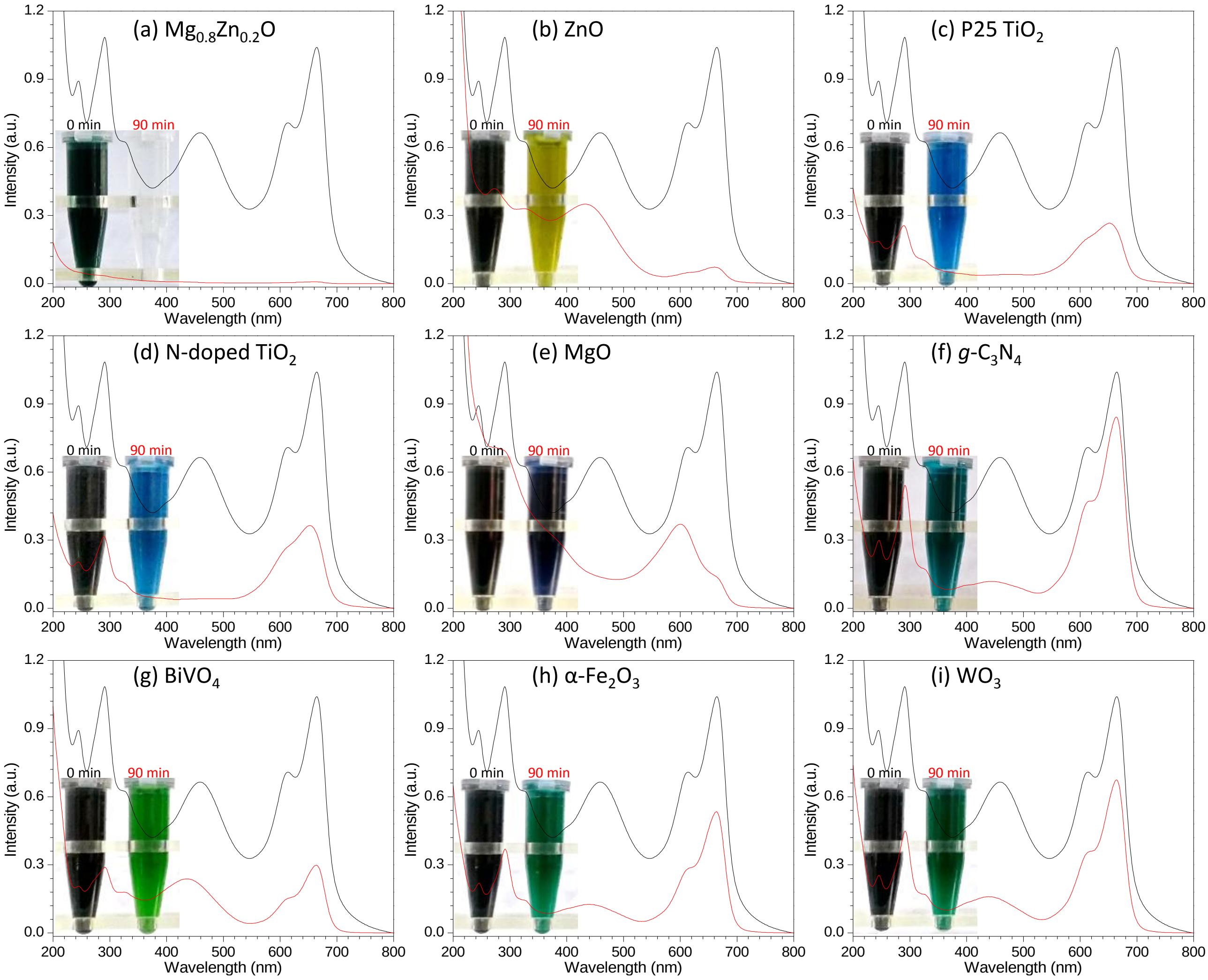

Figure S6. *UV-vis spectra of 50 mL mixed solution (MB, Congo red, thymol blue, bromothymol blue, and eriochrome black T) with each dye concentration of 300 mg L^{-1} being treated with different catalysts:* ***(a)*** *spherical $Mg_{0.8}Zn_{0.2}O$,* ***(b)*** *ZnO,* ***(c)*** *P25 TiO_2,* ***(d)*** *N-doped TiO_2,* ***(e)*** *MgO,* ***(f)*** *g-C_3N_4,* ***(g)*** *$BiVO_4$,* ***(h)*** *α-Fe_2O_3, and* ***(i)*** *WO_3 upon UV light irradiation (— means the solution before treatment, and — means the solution after treatment with 90 min; insets are the photographic images of the corresponding solutions after 0 min and 90 min; catalyst amount: 25 mg).*

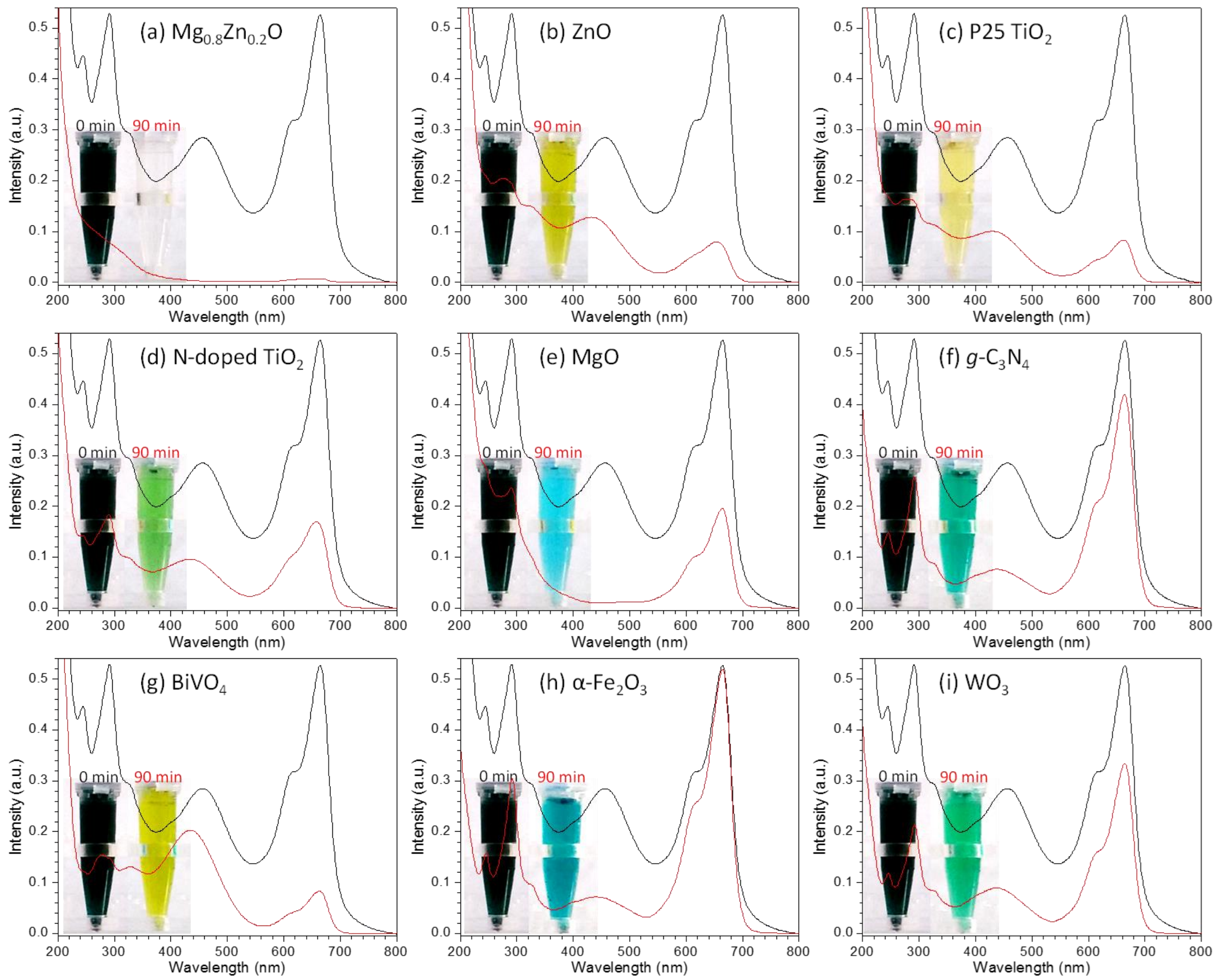

Figure S7. *UV-vis spectra of 50 mL mixed solution (MB, Congo red, thymol blue, bromothymol blue, and eriochrome black T) with each dye concentration of 100 mg L^{-1} being treated with different catalysts:* ***(a)*** *spherical $Mg_{0.8}Zn_{0.2}O$,* ***(b)*** *ZnO,* ***(c)*** *P25 TiO_2,* ***(d)*** *N-doped TiO_2,* ***(e)*** *MgO,* ***(f)*** *g-C_3N_4,* ***(g)*** *$BiVO_4$,* ***(h)*** *α-Fe_2O_3, and* ***(i)*** *WO_3 upon visible light irradiation (— means the solution before treatment, and — means the solution after treatment with 90 min; insets are the photographic images of the corresponding solutions after 0 min and 90 min; catalyst amount: 50 mg).*

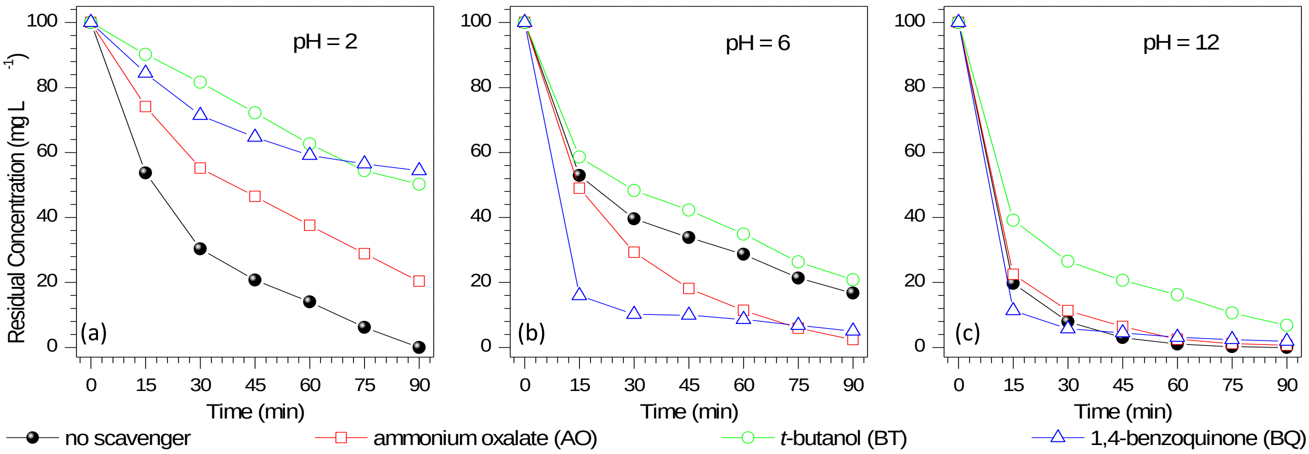

Figure S8. Effects of different scavengers on the photocatalytic degradation of methylene blue percentage over developed $Mg_{0.8}Zn_{0.2}O$ under visible light irradiation with variation in pH values of methylene blue aqueous solutions: (a) pH 2, (b) pH 6, and (c) pH 12 [initial concentration of methylene blue solution: 100 mg L^{-1}; volume: 50 mL; catalytic period: 90 min; catalyst amount: 50 mg; to study the roles of different active species, ammonium oxalate (AO, 5.0 mmol L^{-1}), t-butanol (BT, 5.0 mmol L^{-1}), and 1,4-benzoquinone (BQ, 1.0 mmol L^{-1}) were the scavengers for holes (h^+), hydroxyl radicals ($\bullet OH$), and superoxide radicals ($O_2^{\bullet -}$), respectively].

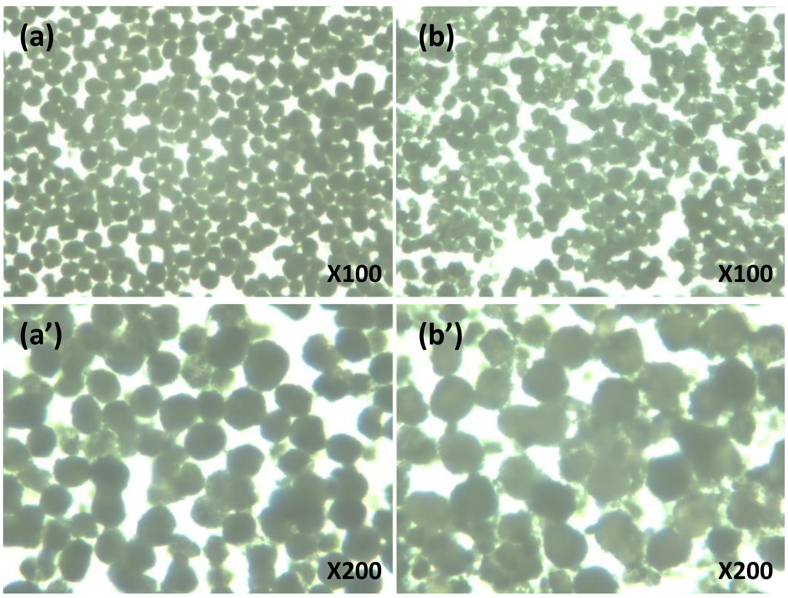

Figure S9. *Optically microscopic images of* ***(a)*** *and* ***(a’)*** *as-synthesized* $Mg_{0.8}Zn_{0.2}O$ ***(b)*** *without use and* ***(b’)*** *the collected product after one cycle for degrading 100 mg* L^{-1} *of methylene blue solution with pH = 2 upon irradiation in visible light.*

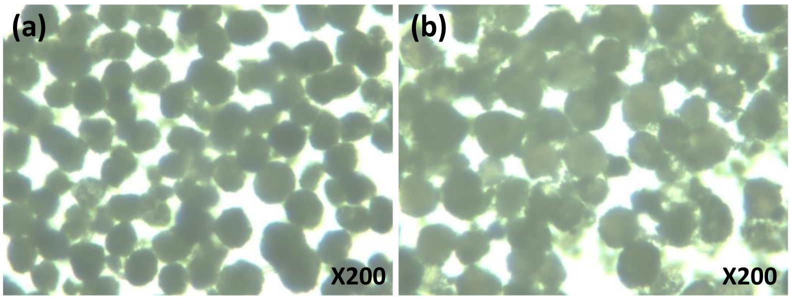

Figure S10. *Optically microscopic images of* ***(a)*** *as-synthesized* $Mg_{0.8}Zn_{0.2}O$ *without use and* ***(b)*** *the collected product after six recycles for degrading 100 mg* L^{-1} *of methylene blue solution upon irradiation in visible light.*

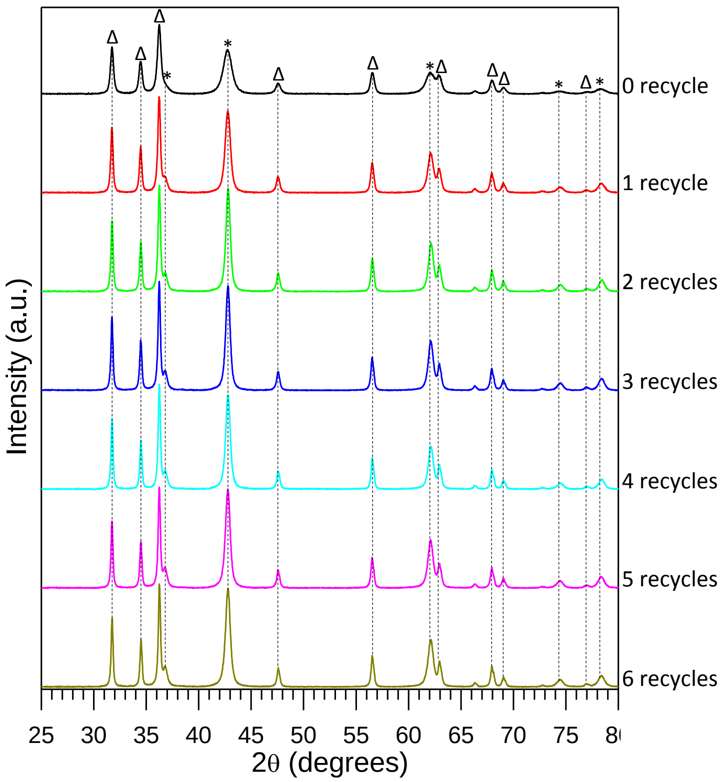

Figure S11. *XRD patterns of recycled products as indicated in this figure (note: * means the diffraction peaks of MgO, and Δ means the diffraction peaks of ZnO in the products).*

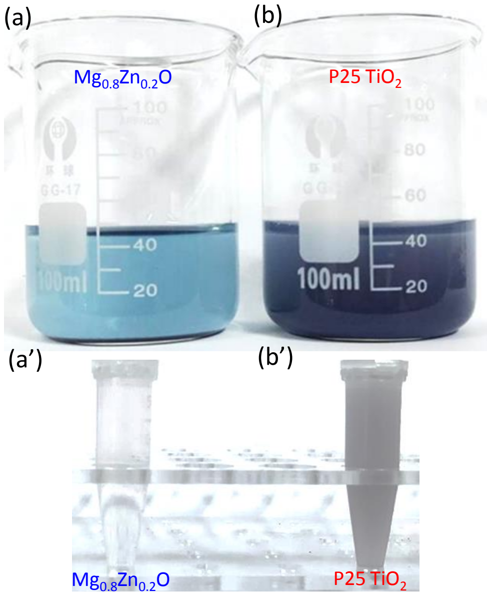

Figure S12. *Photographic images of 50 mL of 100 mg L^{-1} methylene blue solution after being treated with visible light irradiation for 90 min in the presence of* ***(a)*** *$Mg_{0.8}Zn_{0.2}O$ and* ***(b)*** *P25 TiO_2 (after photocatalysis, the solutions have been maintianed constant for 30 min without any stirring), and the supernatant solutions from the systems with* ***(c)*** *$Mg_{0.8}Zn_{0.2}O$ and* ***(d)*** *P25 TiO_2 (catalyst amount: 50 mg).*

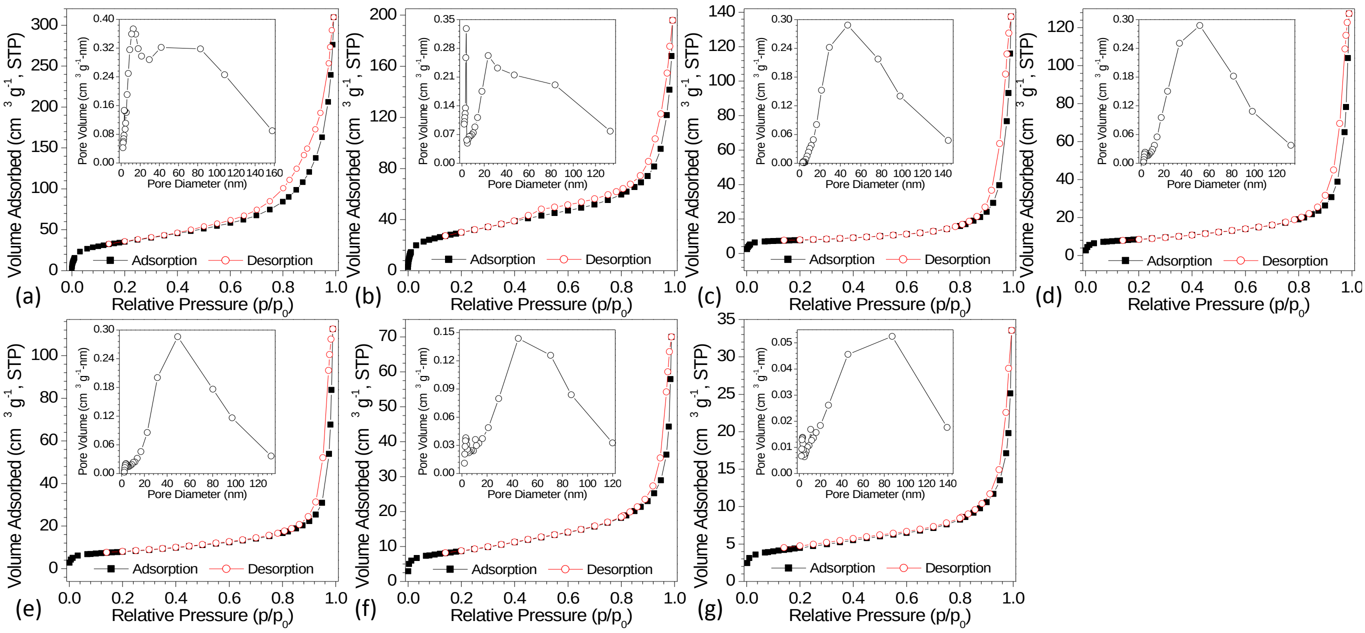

Figure S13. N_2 adsorption–desorption isotherms and pore size distributions (insets) of the generated product with different Mg/Zn ratios: **(a)** MgO, **(b)** $Mg_{0.9}Zn_{0.1}O$, **(c)** $Mg_{0.8}Zn_{0.2}O$, **(d)** $Mg_{0.7}Zn_{0.3}O$, **(e)** $Mg_{0.5}Zn_{0.5}O$, **(f)** $Mg_{0.2}Zn_{0.8}O$, and **(g)** ZnO.

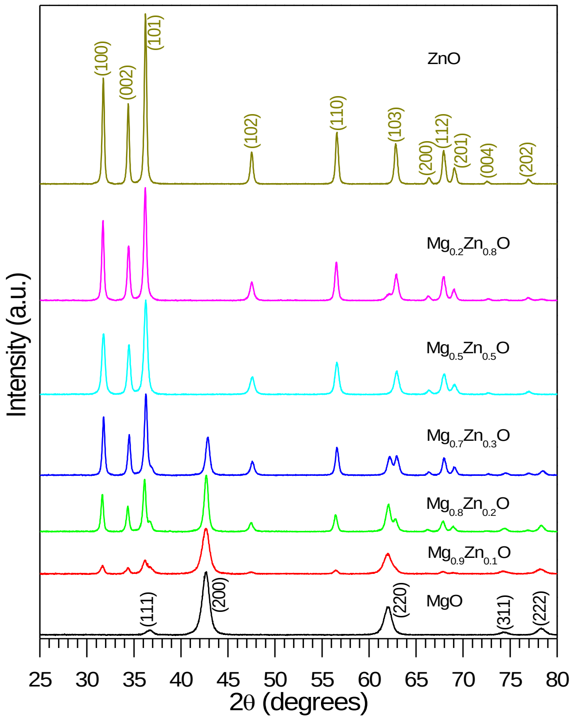

Figure S14. *XRD patterns of the generated products with different Mg/Zn ratios as indicated in this figure.*

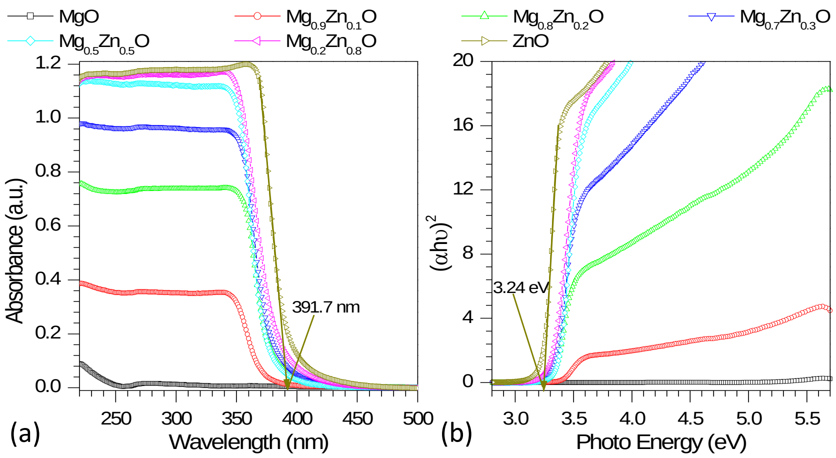

Figure S15. (a) *UV DRS and **(b)** plot of $(\alpha h\upsilon)^2$ vs $(h\upsilon)$ of the generated products with different Mg/Zn ratios as indicated in this figure.*

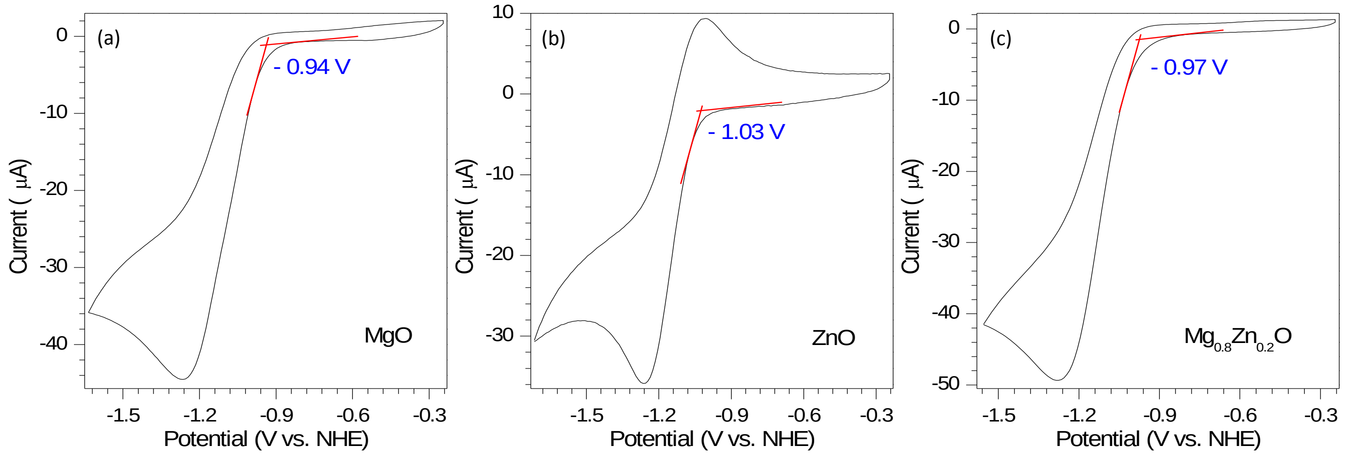

Figure S16. Cyclic voltammetry measurement for **(a)** MgO, **(b)** ZnO, and **(c)** $Mg_{0.8}Zn_{0.2}O$.

Table S1. Comparison of different Mg/Zn binary oxides in degradation of organic dyes or others

Mg/Al oxides	light	solution volume	catalyst dosage	dye	concentration	Reference
$Mg_{0.8}Zn_{0.2}O$ microspheres	UV light	50 mL	25 mg	methylene blue, Congo red, thymol blue, bromothymol blue, eriochrome black T and their mixtures	300 mg/L	**current work**
	visible light	50 mL	50 mg		100 mg/L	
$Mg_{0.5}Zn_{0.5}O$ nanoparticles	UV light	250 mL	60 mg	indigo carmine	40 mg/L	[1]
$Mg_{0.8}Zn_{0.2}O$ nanoparticles	UV light	200 mL	50 mg	methyl orange	20 mg/L	[2]
$Mg_{0.3}Zn_{0.7}O$ thin film	UV light	100 mL	n/a	crystal violet	20 mg/L	[3]
$MgO/ZnO/In_2O_3$ nanoparticles	Visible light	100 mL	50 mg	methylene blue	10 mg/L	[4]
$Mg_{0.5}Zn_{0.5}O$ nanoparticles	UV light	50 mL	100 mg	2,6-dichlorophenol	10 mg/L	[5]
MgO/ZnO nanoparticles	UV light	20 mL	20 mg	alprazolam	9 mg/L	[6]
$Mg_{0.904}Zn_{0.096}O$ nanoparticles	UV light	50 mL	3 mg	methylene blue	6 mg/L	[7]
$Mg_{0.05}Zn_{0.95}O$ nanoparticles	UV light	80 mL	50 mg	methylene blue	6 mg/L	[8]
$Mg_{0.05}Zn_{0.95}O$ nanoparticles	blacklight	150 mL	150 mg	methylene blue	3 mg/L	[9]
$Mg_{0.10}Zn_{0.80}C_{0.10}$ nanoparticles	UV light	100 mL	100 mg	methylene blue	3 mg/L	[10]
$Mg_{0.10}Zn_{0.90}O$ nanoparticles	sunlight	50 mL	60 mg	methylene blue	3 mg/L	[11]
$Mg_{0.05}Zn_{0.95}O$ nanoparticles	blacklight	150 mL	150 mg	methylene blue	3 mg/L	[12]

Note: n/a means not available.

Table S2. Comparison of different types of MgO in degradation of organic dyes

Mg/Al oxides	light	solution volume	catalyst dosage	dye	concentration	Reference
$Mg_{0.8}Zn_{0.2}O$ microspheres	UV light	50 mL	25 mg	methylene blue, Congo red, thymol blue, bromothymol blue, eriochrome black T and their mixtures	300 mg/L	**current work**
	visible light	50 mL	50 mg		100 mg/L	
MgO microspheres	UV light	20 mL	10 mg	methylene blue, Congo red, thymol blue, bromothymol blue, eriochrome black T and their mixture	100 mg/L	[13]
MgO nanorods	visible light	150 mL	2 mg	methylene blue	25 mg/L	[14]
MgO nanoparticles	UV light	250 mL	60 mg	methylene blue	20 mg/L	[15]
MgO nanoparticles	UV light	100 mL	50 mg	methyl orange and methylene blue	15 mg/L	[16]
MgO nanospheres	UV light	50 mL	4 mg	indigo carmine	15 mg/L	[17]
MgO nanoflake	UV light	100 mL	200 mg	methyl orange	10 mg/L	[18]
MgO nanoflake	UV light	25 mL	10 mg	methylene blue	10 mg/L	[19]
MgO nanofibre	UV light	5 mL	20 mg	reactive yellow	10 mg/L	[20]
MgO nanoparticles	UV light	50 mL	50 mg	methylene blue, methyl orange, acid orange 7 and rhodamine 6G	5 mg/L	[21]
MgO nanoparticles	UV light	30 mL	50 mg	methylene blue	1.8 mg/L	[22]

Table S3. Texture properties of different Mg/Zn binary oxides

Mg/Zn oxides	specific surface area[a] (m^2 g^{-1})	average pore diameter[b] (nm)	pore volume (cm^3 g^{-1})	crystallite size[c] (nm)	band gap energy[d] (eV)
MgO	127.6	13.6	0.48	8.80	5.24
$Mg_{0.9}Zn_{0.1}O$	108.3	11.0	0.31	8.50	3.40
$Mg_{0.8}Zn_{0.2}O$	26.5	34.2	0.21	4.27	3.34
$Mg_{0.7}Zn_{0.3}O$	29.9	25.7	0.20	3.78	3.34
$Mg_{0.5}Zn_{0.5}O$	27.8	27.4	0.17	3.63	3.37
$Mg_{0.2}Zn_{0.8}O$	30.5	15.2	0.11	2.62	3.32
ZnO	15.6	17.7	0.05	3.96	3.24

Note: [a] Using the standard Brunauer–Emmett–Teller (BET) method. [b] Using the Barret–Joyner–Halenda (BJH) method. [c] Using the Debye–Scherrer formula based on the full width at half-maximum (fwhm) of the (200) plane. [d] Estimated from UV diffused reflectance spectroscopy (DRS).

Table S4. The kinetic parameters of ZnO, MgO and $Mg_{0.8}Zn_{0.2}O$ from their time profiles using the fitting line of Lorentzian function

oxides	y_0	A	W	τ_0 (ns)
ZnO	0	68930.6	17.79	198.7
MgO	0	59634.2	60.70	195.7
$Mg_{0.8}Zn_{0.2}O$	0	64184.1	64.80	193.6

Note: Lorentzian function is below.

$$y(t) = y_0 + \frac{2A}{\pi}\left[\frac{W}{4(t-\tau_0)^2 + W^2}\right]$$

References

(1) M. Sangeeta, K. V. Karthi, R. Ravishankar, K. S. Anantharaju, H. Nagabhushana, K. Jeetendra, Y. S. Vidya and L. Renuka, *Mater. Today-Process.*, 2017, **4**, 11791-11798.

(2) J. Lian, C. Zhang, Q. Li and D. H. L. Ng, *Nanoscale*, 2013, **5**, 11672-11678.

(3) M. Boshta, M. O. Abou-Helal, D. Ghoneim, N. A. Mohsen and R. A. Zaghlool, *Surf. Coat. Technol.*, 2010, **205**, 271-274.

(4) X. Xiang, L. S. Xie, Z. W. Li and F. Li, *Chem. Eng. J.*, 2013, **221**, 222-229.

(5) A. I. Vaizogullar, *Kinet. Catal.*, 2018, **59**, 418-427.

(6) T. B. Ivetić, M. R. Dimitrievska, N. L. Finčur, L. R. Đačanin, I. O. Gúth, B. F. Abramović and S. R. Lukić-Petrović, *Ceram. Int.*, 2014, **40**, 1545-1552.

(7) A. Sierra-Fernandez, S. C. De la Rosa-Garcia, L. S. Gomez-Villalba, S. Gomez-Cornelio, M. E. Rabanal, R. Fort and P. Quintana, *ACS Appl. Mater. Inter*., 2017, **9**, 24873-24886.

(8) X. Qiu, L. Li, J. Zheng, J. Liu, X. Sun and G. Li, *J. Phys. Chem. C*, 2008, **112**, 12242-12248.

(9) S. Klubnuan, P. Amornpitoksuk and S. Suwanboon, *Mater. Sci. Semicond. Process.*, 2015, **39**, 515-520.

(10) M. A. Karimi, A. Hatefi-Mehrjardi, A. A. Kabir and M. Zaydabadi, *Res. Chem. Intermed.*, 2015, **41**, 6157-6168.

(11) V. Etacheri, R. Roshan and V. Kumar, *ACS Appl. Mater. Interfaces*, 2012, **4**, 2717-2725.

(12) S. Suwanboon, P. Amornpitoksuk, P. Bangrak and N. Muensit, *Ceram. Int.*, 2013, **39**, 5597-5608.

(13) Y. Zheng, L. Cao, G. Xing, Z. Bai, J. Huang and Z. Zhang, *RSC Adv.*, 2019, **9**, 7338-7348.

(14) N. Salehifar, Z. Zarghami and M. Ramezani, *Mater. Lett.*, 2016, **167**, 226-229.

(15) K. N. S. Kumara, H. P. Nagaswarupa, K. R. V. Mahesh, S. C. Prashantha, M. Mylarappa and D. M. K. Siddeshwara, *Nanosyst.-Phys. Chem. Math.*, 2016, **7**, 662-666.

(16) K. Mageshwari, S. S. Mali, R. Sathyamoorthy and P. S. Patil, *Powder Technol.*, 2013, **249**, 456-462.

(17) A. B. Gh, M. Sabbaghan and Z. Mirgani, *Spectroc. Acta Pt. A-Molec. Biomolec. Spectr.*, 2015, **137**, 1286-1291.

(18) R. Sathyamoorthy, K. Mageshwari, S. S. Mali, S. Priyadharshini and P. S. Patil, *Ceram. Int.*, 2013, **39**, 323-330.

(19) A. Najafi, *Ceram. Int.*, 2017, **43**, 5813-5818.

(20) M. Mantilaka, R. T. De Silva, S. P. Ratnayake, G. Amaratunga and K. M. N. de Silva, *Mater. Res. Bull.*, 2018, **99**, 204-210.

(21) M. Y. Guo, A. M. C. Ng, F. Liu, A. B. Djurišić and W. K. Chan, *Appl. Catal. B*, 2011, **107**, 150-157.

(22) S. Demirci, B. Ozturk, S. Yildirim, F. Bakal, M. Erol, O. Sancakoglu, R. Yigit, E. Celik and T. Batar, *Mater. Sci. Semicond. Process*, 2015, **34**, 154-161.